Electrochimica Acta 96 (2013) 1–7

Contents lists available at SciVerse ScienceDirect

Electrochimica Acta

journal homepage: www.elsevier.com/locate/electacta

Simple model of mass transfer in template synthesis of metal ordered nanowire arrays

Daniil A. Bograchev[a], Vladimir M. Volgin[b,1], Alexey D. Davydov[a,*,1]

[a] Frumkin Institute of Physical Chemistry and Electrochemistry, Russian Academy of Sciences, Leninskii pr. 31, Moscow 119071, Russia
[b] Tula State University, pr. Lenina 92, Tula 300600, Russia

ARTICLE INFO

Article history:
Received 10 December 2012
Received in revised form 15 February 2013
Accepted 15 February 2013
Available online 24 February 2013

Keywords:
Metal electrodeposition
Anodic aluminum oxide
Nanowires
Template synthesis

ABSTRACT

A simple model of electrochemical growth of nanowires in the pores of anodic aluminum oxide (AAO) template is developed. The metal deposition is considered at various overpotentials. The model takes into consideration the ionic transfer both in the varying diffusion layer in the pores and in the diffusion layer above the template, which is determined by the external hydrodynamic conditions. The model takes into account the kinetics of electrochemical reaction by means of the Tafel equation and the diffusion transfer of metal cations both in the pores and in the outer diffusion layer. The analytical solution of the problem with several simplifications yields the equations for calculating the time dependence of current, the pore filling time, and other parameters of the process. An example of the application of the model for the analysis of nanowire growth in the template pores is compared with the experimental data showing good agreement.

1. Introduction

In recent years, a large number of experimental studies have been devoted to the template synthesis of metal (Fe, Ni, Co, various alloys and chemical compounds) ordered nanowire arrays [1–39]. Most frequently, a porous oxide film, which was produced by aluminum anodizing and then separated from the nonporous (barrier) oxide layer and aluminum substrate, is used as the template. A metal (copper, gold) layer is spayed in vacuum onto one side of porous film. The layer serves as the current lead in the metal deposition into the oxide film pores. The porous layer is commonly 50 μm thick, the pores are 40–50 nm in diameter (high aspect ratio pores), and the porosity is $\varepsilon = \pi k r^2 \approx 0.13$ (k is the number of pores per unit surface area of specimen and r is the pore radius). The pores are spaced approximately 100 nm apart [7,34].

In some works, nuclear track polycarbonate (polyethylene terephthalate, mica) membranes were used as the templates [5,28,30,36,40]. In these cases, the membranes were 5–20 μm thick and the pores were 10–500 nm in diameter. A pore density was $2–6 \times 10^8$ cm^{-2} [4,30] and 1.05×10^{10} cm^{-2} [34]). Porous silicon was also used as the template with the pores 10–60 nm in diameter and 10–30 μm in length [9].

A porous film with a metal layer (current lead) is placed into an electrochemical cell and serves as the cathode. Commonly, a three-electrode cell is used. The pores are filled with a metal in the corresponding electrolyte (for example, in the Watts bath for nickel deposition), frequently, under the potentiostatic conditions.

Great interest in these systems is associated with their potential application in the fields of high-density magnetic memories, optoelectronic devices, nanoscale electronics, electromechanical devices, catalytically active electrodes for the analysis of solution composition, etc.

Based on Refs. [28,30,34,36], we can recognize at least three main stages of pore filling with metal (Fig. 1).

(1) A stage of non-steady-state diffusion. When a potential is applied, the current increases abruptly and, then, decreases with time in accordance with the diffusion layer thickness increasing from zero to the porous layer thickness. Here, the Cottrell equation is valid.
(2) A stage of pore filling with metal. Thereby, the current slightly increased, remained invariant, or even slightly decreased with time in different works. The duration of this stage (t_{fill}) is much longer than that of the first stage.
(3) The pores are filled up, the metal wires emerge from the pores. The effective cathode surface area increases, the current steeply increases. When the entire surface is coated with the metal film, the current reaches a certain constant value.

It should be noted that the current and pore filling time t_{fill} depend on the potential [7,28,36]: the higher the potential (the overpotential of cathodic reaction), the higher the current and shorter the time t_{fill}.

* Corresponding author. Tel.: +7 495 9547216.
E-mail addresses: davydov@elchem.ac.ru, alexdavydov@ya.ru (A.D. Davydov).
[1] ISE member.

0013-4686/$ – see front matter © 2013 Elsevier Ltd. All rights reserved.
http://dx.doi.org/10.1016/j.electacta.2013.02.079

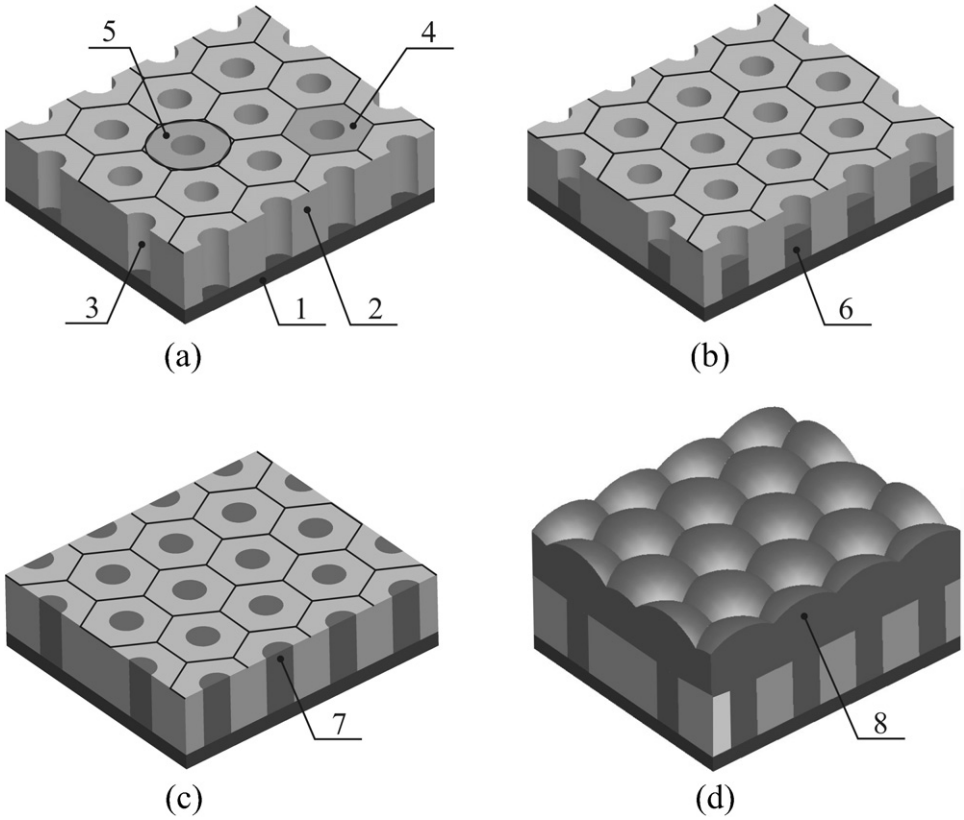

Fig. 1. A scheme of template metal electrodeposition into AAO. (a) The template prior to the metal deposition; (b) the template with partially filled pores; (c) the template with completely filled pores; and (d) the template coated with continuous layer of metal deposit. (1) Conducting layer, (2) template, (3) a pore, (4) template surface area corresponding to a single pore, (5) axisymmetric approximation of the template surface area corresponding to a single pore, (6) a nanowire that partly fills the pore, (7) a nanowire that completely fills a pore, and (8) continuous layer of metal deposit on the template surface.

The majority of published works on this problem are the experimental studies. They show that nanowires can be produced by the cathodic deposition of various metals and some substances into the pores, predominantly, in AAO.

Only a few theoretical studies on this problem are available. For example, the authors of [4] developed and simulated a 2D model for the electrodeposition of metal inside the porous AAO template, which deals with one only potentiostatic pulse applied to one pore.

The transfer processes in the electrodeposition of cobalt into the pores (250 nm in diameter and 20 μm in length) of nuclear track polycarbonate membranes at the limiting current were theoretically analyzed in [17]. Two periods were considered: a short period of non-steady-state diffusion, when the Cottrell equation is valid, and a longer period, when gradually increasing radii of spherically shaped diffusion zones from each recessed nanoelectrode result in the overlapping of diffusion zones, and, finally, a constant steady-state limiting current was reached.

The aim of the work is to develop an approximate method for simulating mass transfer and nanowire growth in the template pores with regard for the kinetics of electrode reaction and diffusion limitations both in the pores and diffusion layer of electrolyte above the template surface. The problem will be solved analytically and the equations for calculating the time dependence of metal deposition current, the pore filling time, and other parameters of the process will be obtained.

2. Statement of problem

In the work, it is assumed that the pores in the template are arranged regularly (Fig. 1a), and a region of electrolyte solution between the template surface and anode with a regular hexagonal cross-section (4 in Fig. 1a) corresponding to each pore can be approximated by the region with round cross-section (5 in Fig. 1a). The shape of cross-section has an effect on the mass transfer only in the transient zone II (Fig. 2b); its length does not exceed several distances between the pores. The diffusion transfer in zone II is estimated by the finite element method for the system's parameters (porosity, pore radius, pore length, the distance from the template to the anode) of practical importance. It is shown that an error due to axisymmetric approximation does not exceed 1%. The use of axisymmetric approximation enables one to reduce a 3D problem to 2D one and, consequently, simplify the numerical solution with an insignificant loss of accuracy. Therefore, hereafter, the axisymmetric approximation is used. The radius of the region with round cross-section was determined by the following equation:

$$R = r_p\sqrt{\varepsilon} \tag{1}$$

Fig. 2 gives a scheme of calculating the mass transfer in the axisymmetric region. Here, d is the porous film (template) thickness (the initial pore length); d^* is the current thickness of deposit layer in the pore; $L = d - d^*(t)$ is the current thickness of layer free of metal in the pore; r_p is the pore radius; R is the radius of axisymmetric region corresponding to a single pore; δ is the thickness of outer diffusion layer determined by the external hydrodynamic conditions; c_0, c_p, and c_s are the concentrations of metal cations in the bulk solution, at the pore bottom, and an average concentration in the pore mouth, respectively; I is a zone in the pore with 1D distribution of concentration; II is a transient zone with 2D distribution of concentration; III is a zone in the solution with 1D distribution of concentration; I′ and III′ are approximations of zones I and III, respectively.

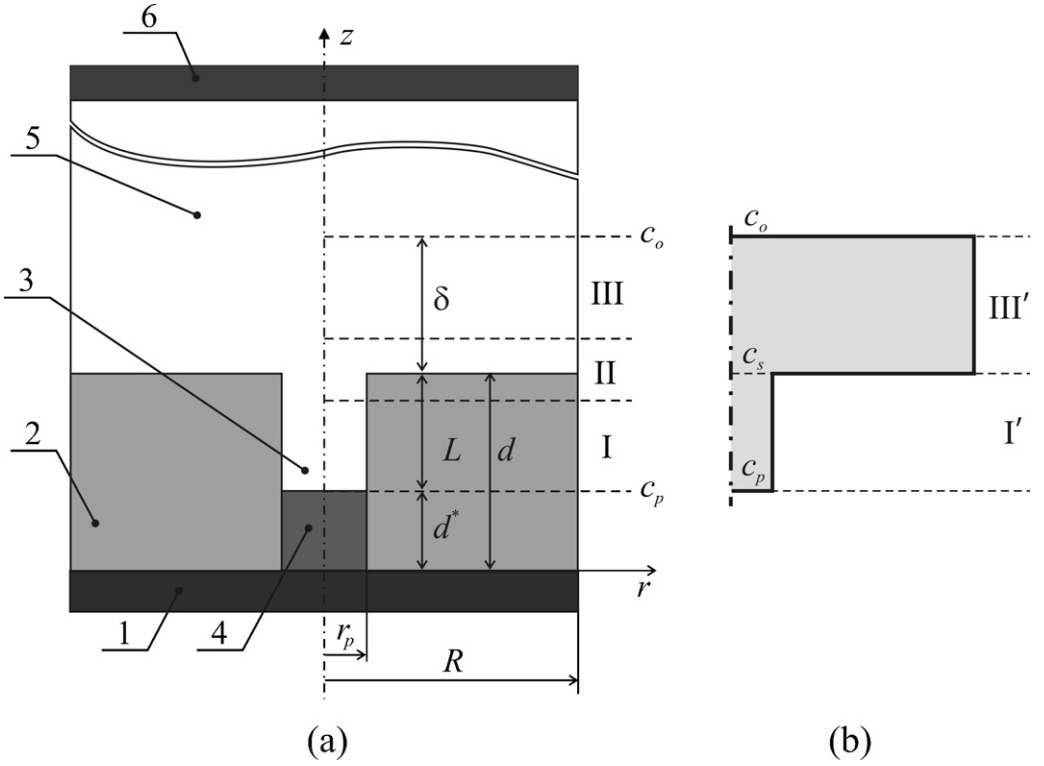

Fig. 2. A scheme for calculating the mass transfer in the metal deposition in a pore. (1) A conducting layer (current lead), (2) template, (3) a pore, (4) a pore portion filled with metal, (5) a space between the template and auxiliary electrode filled with the electrolyte, and (6) an auxiliary electrode (anode).

In the general case, at the distances more than r_p from the outer template surface, the distribution of concentration is almost independent of the radial coordinate [41], i.e. it is 1D (zones I and III). At smaller distances, the distribution of concentration depends both on the vertical coordinate and radius, i.e. it is 2D (zone II). However, these distances are by several orders of magnitude smaller than the pore length. Therefore, in the model, the distribution of concentration over the radius is ignored throughout the pore length (from the bottom to the mouth).

The model takes into account the time-varying diffusion layer L, which is equal to the unfilled part of a pore, and the outer diffusion layer with a constant thickness δ determined by the external hydrodynamic conditions (the solution was stirred).

Within this approximation, the calculation of mass transfer is reduced to the solution of 1D problem in the pore with moving lower boundary (I′) and axisymmetric problem in the region between the outer template surface and outer boundary of diffusion layer (region III′). The concentration in the pore mouth (at the boundary between I′ and III′ regions) is not known beforehand and can be determined from the condition of equal diffusion fluxes of electroactive ions in zones I′ and III′ in the pore mouth. In the model, the transfer of only electroactive ions, i.e. metal cations, is taken into account.

In this work, we consider only the second stage of pore filling with metal in the solution containing metal cations with concentration c_0. This choice is based on the fact that the first stage (non-steady-state diffusion) is much shorter than the second one, the pore filling with metal proceeds almost completely at the second stage. (Simple estimation of the time of diffusion front propagation from the pore bottom to its mouth d^2/D, where D is the diffusion coefficient of metal cations in the pore, and the experimental results, for example [34], show that the first stage is by approximately two orders of magnitude shorter than the second stage.) The third stage (the wires emerge from the template surface) lies beyond the scope of practical problem: the template synthesis of metal ordered nanowire arrays.

Assume that, at the first stage, the metal deposition proceeds under the mixed (non-steady-state diffusion and charge-transfer) control. By the end of the first stage, the quasi-steady-state concentration of cations at the pore bottom is reached. This concentration of cations and current depend on the prescribed overpotential, the initial concentration of electroactive ions, their diffusion coefficient, and pore length.

Further variations in the quasi-steady-state concentration of cations and current are determined by the conditions of steady-state diffusion and the kinetic Tafel equation.

The used condition $(d - d^*(t)) \gg r_p$ is valid for the metal deposition in the AAO templates, except for the last short period of pore filling.

3. Solution of problem

Under the above assumptions, the problem can be reduced to two conjugated quasi-steady-state problems: axisymmetric problem with partially insulated surface and 1D problem in a pore with varying length.

The solutions of the problems are given below.

3.1. Axisymmetric problem with partially insulated surface. A flux of electroactive ions in zone III′

A flux of electroactive ions in zone III′ was determined as a result of numerical solution of diffusion equation in the axisymmetric region with height δ and outer radius R (Fig. 2):

$$\frac{\partial^2 c}{\partial r^2} + \frac{1}{r}\frac{\partial c}{\partial r} + \frac{\partial^2 c}{\partial z^2} = 0, \tag{2}$$

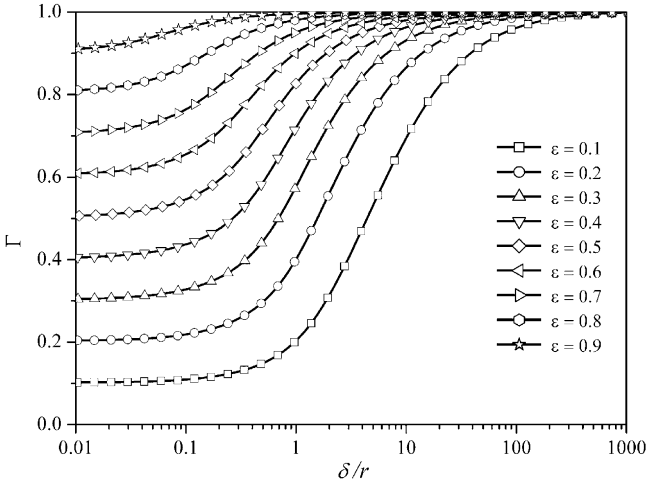

Fig. 3. The plots of geometric factor Γ vs. the ratio of outer diffusion layer thickness to the pore radius at various template porosities ε.

with the following boundary conditions:

$$c|_{z=d+\delta} = c_0, \tag{3}$$

$$c|_{z=d,r<R_p} = 0, \tag{4}$$

$$\left.\frac{\partial c}{\partial n}\right| = 0. \tag{5}$$

A difference between the concentrations at the upper boundary of diffusion layer δ and the concentration in the pore mouth was taken to be c_0 (Eqs. (3) and (4)), other regions of the boundary were considered as nonconductive (5).

To elucidate the question whether a partial insulation of template surface has an effect on the mass-transfer rate in zone III′, a parameter Γ was introduced. It is a ratio between the electroactive ion flux to the electrode with partially insulated surface and that to the uninsulated electrode:

$$\Gamma = \frac{2\delta\int_0^{r_p} r(\partial c/\partial z)dr}{c_0 R^2} = \frac{2\delta\int_0^{r_p} r(\partial c/\partial z)dr}{c_0 {r_p}^2 \varepsilon} \tag{6}$$

The results of numerical solution of the problem (Fig. 3) showed that, if the diffusion layer thickness δ is much larger than the pore radius and the distance between the pores, Γ is approximately unity and partial insulation of surface has no noticeable effect on the mass-transfer rate.

Using parameter Γ, an average current density $\bar{j}$ in zone III′ can be determined by the following equation:

$$\bar{j} = \frac{\Gamma\gamma nFD(c_0 - c_s)}{\delta} \tag{7}$$

where D is the diffusion coefficient of electroactive cations in a template pore; n is the charge of cation; F is the Faraday's constant; γ is a ratio of diffusion coefficient of cations in the "free electrolyte" to that in a pore.

The coefficient γ was introduced, because the authors of several experimental studies [7,34,38,39] concluded that the diffusion of cations in the pores of anodic oxide film is suppressed as compared to bulk diffusion; for example, according to [34], the diffusion coefficient of nickel cations in a pore is approximately 2.0×10^{-7} cm^2/s against 6×10^{-6} cm^2/s in the bulk solution. If the diffusion coefficients in zones I′ and III′ are equal, $\gamma = 1$.

3.2. 1D problem in a pore with varying length

In 1D approximation, for the diffusion current density in a single pore j_p, we can write (see Fig. 2):

$$j_p = \frac{nDF(c_s - c_p)}{L}. \tag{8}$$

Due to the conservation law, the current density $\bar{j}$ averaged over the surface of specimen with a system of pores can be expressed in terms of current density in a single pore and porosity ε:

$$\bar{j} = j_p\varepsilon. \tag{9}$$

The current j_p can be related to the charge-transfer overpotential η by using the Tafel equation:

$$j_p = j_0\frac{c_p}{c_0}\exp\left(-\frac{\alpha F\eta}{RT}\right), \tag{10}$$

where j_0 is the exchange current density, α is the transfer coefficient, R is the gas constant, and T is the temperature.

From (10), the concentration at the pore bottom can be expressed as a function of current:

$$c_p = \frac{c_0 j_p}{j_0}\exp\left(\frac{\alpha F\eta}{RT}\right). \tag{11}$$

The current is related to the deposited metal thickness by the Faraday's equation:

$$d^*(t) = \frac{M}{nF\rho_M}\int_0^t j_p dt, \tag{12}$$

where M is the molar weight of metal and ρ_M is the metal density. It is assumed that the current efficiency for the metal deposition is 100% and all pores are filled concurrently. (In some experimental works, for example [7,22,28,36], it was shown that this condition is fulfilled under certain conditions.)

Then, for the current density in a single pore:

$$j_p = -\frac{nF\rho_M}{M}\frac{\partial L}{\partial t} \tag{13}$$

In view of Eqs. (8), (11) and (13), and also Eqs. (7), (9) and (13) the system of Eqs. (14) and (15) describing pore filling is as follows:

$$\frac{\partial L}{\partial t} = -\frac{MD(c_s + (nF\rho_M c_0/j_0 M)(\partial L/\partial t)\exp(\alpha F\eta/RT))}{\rho_M L} \tag{14}$$

$$\frac{\partial L}{\partial t} = -\frac{\gamma\Gamma MD(c_0 - c_s)}{\varepsilon\rho_M\delta} \tag{15}$$

Multiplying (14) by L and (15) by $\varepsilon\delta/\Gamma\gamma$ and combining thus obtained equations, we eliminate the concentration of electroactive ions in the pore mouth c_s from Eqs. (14) and (15). Denote $\delta^* = (nFc_0D/j_0)\exp(\alpha F\eta/RT)$; δ^* can be formally imagined as an additional pore length (additional diffusion layer thickness). Then, we obtain a differential equation describing pore filling with the metal:

$$\frac{\partial L}{\partial t} = -\frac{MDc_0}{\rho_M(L + (\varepsilon\delta/\Gamma\gamma) + \delta^*)}. \tag{16}$$

The parameter δ^* is associated with the Tafel kinetics of metal deposition. When the current tends to the limiting one, this fictitious additional layer thickness tends to zero.

The initial condition for differential Eq. (16) is determined by the porous film thickness d:

$$L\big|_{t=0} = d. \tag{17}$$

Eq. (16) is easily integrated; finally, in view of initial condition (17), the time dependence of L is as follows:

$$L = -\left(\frac{\varepsilon\delta}{\Gamma\gamma} + \delta^*\right) + \sqrt{\left(\frac{\varepsilon\delta}{\Gamma\gamma} + \delta^* + d\right)^2 - 2\frac{MDc_0}{\rho_M}t}. \quad (18)$$

Substituting (18) into (13), we obtain the time dependence of current density in a single pore provided that the deposit thickness does not exceed d:

$$j_p = -\frac{nF\rho_M}{M}\frac{\partial L}{\partial t} = \frac{nFDc_0}{\sqrt{(\delta^* + d + (\varepsilon\delta/\gamma\Gamma))^2 - 2(MDc_0/\rho_M)t}} \quad (19)$$

or, finally, for an average current density:

$$\bar{j} = \frac{\varepsilon nFDc_0}{\sqrt{((nFc_0D/j_0)\exp(\alpha F\eta/RT) + d + (\varepsilon\delta/\gamma\Gamma))^2 - 2(MDc_0/\rho_M)t}} \quad (20)$$

It is seen that within the framework of the model, the current can increase with time, if the denominator decreases.

The pore filling time t_{fill} can be determined from the condition $L = 0$ and (18):

$$t_{fill} = \frac{\rho_M d((\varepsilon\delta/\gamma\Gamma) + (nFc_0D/j_0)\exp(\alpha F\eta/RT)) + d/2)}{MDc_0} \quad (21)$$

The time dependence of concentration at the pore bottom can be determined from (19) and (11):

$$c_p = \frac{nFDc_0{}^2\exp(\alpha F\eta/RT)}{j_0\sqrt{((nFc_0D/j_0)\exp(\alpha F\eta/RT) + d + (\varepsilon\delta/\gamma\Gamma))^2 - 2(MDc_0/\rho_M)t}}. \quad (22)$$

From (22), two limiting cases can be derived. At high overpotentials, the concentration at the pore bottom will be nearly zero $\lim_{E\to\infty} c_p \to 0$ (the limiting current) throughout the period of metal deposition. At relatively low overpotentials and not very thick outer diffusion layer, concentration c_p becomes approximately equal to the bulk concentration $\lim_{E\to 0} c_p \to c_0$.

4. Results and discussion

The analytical solution (18)–(22) describes the pore filling with metal in AAO. It enables one to estimate the time variation of current density and the pore filling time. The solution can be used for predicting and analysis of experimental data.

The geometric factor Γ (Fig. 3) is required for self-consistency of ion flux through the diffusion layer that is common to all pores. For typical sizes of the systems under consideration, Γ can be taken to be unity.

The outer diffusion layer thickness, which is defined by the hydrodynamic conditions near the template surface, is multiplied by the porosity in all equations. When the porosity tends to zero, the mutual effect of pores vanishes. In the case of a single pore with a nanometer radius and micrometer length $\varepsilon \ll 1$, and, therefore, $(nFc_0D/j_0)\exp(\alpha F\eta/RT) + d \gg (\varepsilon\delta/\gamma\Gamma)$, so that the term, which takes into account the resistance to mass transfer in the outer diffusion layer, may be neglected.

Fig. 4 gives the experimental time dependence of current, which was obtained in [34] for the nickel deposition in an AAO template (curve 4), and three time dependences calculated by Eq. (20) for various overpotentials at the following parameters: $j_0 = 2\times10^{-9}$ A/cm^2; $D = 7.8\times10^{-7}$ cm^2/s; $d = 5\times10^{-3}$ cm; $\delta = 1.4\times10^{-2}$ cm; $M = 60$ g/mol; $\rho = 8.9$ g/cm^3; $\varepsilon = 0.055$; (it was decreased as compared to [34] due to a low filling factor in [34]);

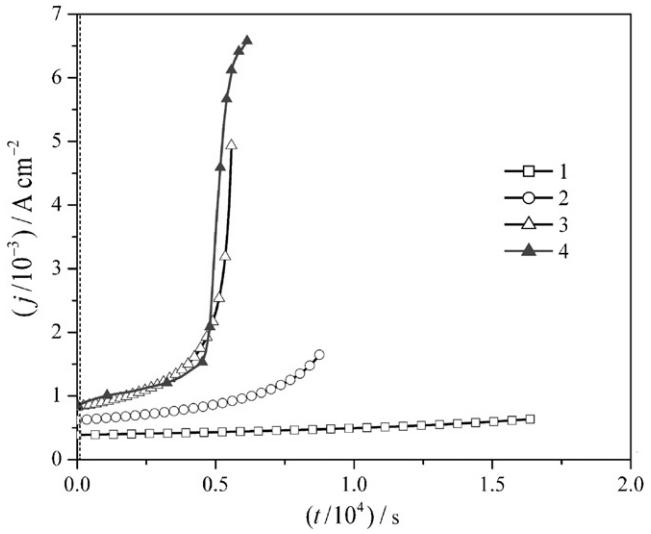

Fig. 4. (1)–(3) Time dependences of current, which were calculated by Eq. (16) at (1) $\eta = -0.8$ V, (2) $\eta = -0.85$ V, and (3) $\eta = -0.91$ V, and (4) the experimental time dependence, which was obtained in [34] for the nickel deposition in an anodic aluminum oxide template. Dashed line corresponds to the end of the first stage.

$c_0 = 0.6\times10^{-3}$ mol/cm^3; $\Gamma = 1$; $\gamma = 7.72$; $\alpha = 0.5$; $\eta = -0.8$ V (curve 1), $\eta = -0.85$ V (curve 2), and $\eta = -0.91$ V (curve 3). Here, j_0 and α were taken from [42] for nickel deposition from 1 M $NiSO_4$ solution.

It is seen that the application of this simple model enables one to calculate the results that agree with the experimental data both in the shape of current vs. time curve and in the pore filling time. It should be noted that, in the model, only a period of deposit growth inside the pores is considered; an abrupt increase of the current in the calculated curve 3 is not associated with the growth of caps at the end of wires. An increase of the current in the calculated curves corresponds to a decrease of the inner diffusion layer thickness at the final stage of deposit growth in the pores. At high overpotentials of electrochemical reaction and intense stirring of solution, the current can increase significantly even before the wires emerge from the template surface.

Fig. 5 shows the time dependences of degree of pore filling at three overpotentials. It is seen that the pore filling time decreases with increasing overpotential. At relatively low overpotential, the dependence is almost linear.

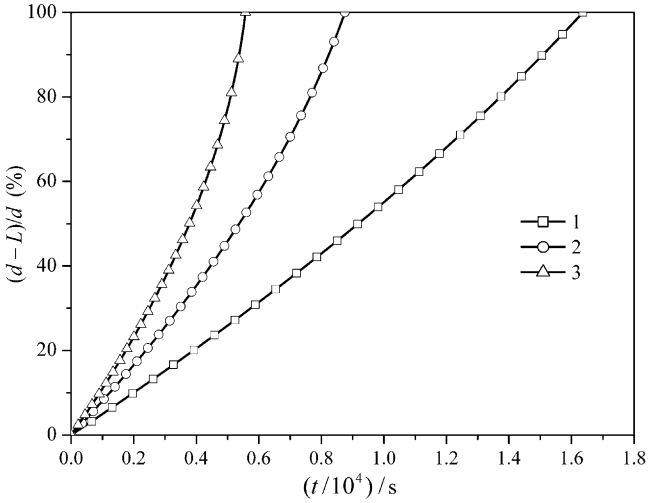

Fig. 5. Time dependences of degree of pore filling at various overpotentials: (1) $\eta = -0.8$ V, (2) $\eta = -0.85$ V, and (3) $\eta = -0.91$ V.

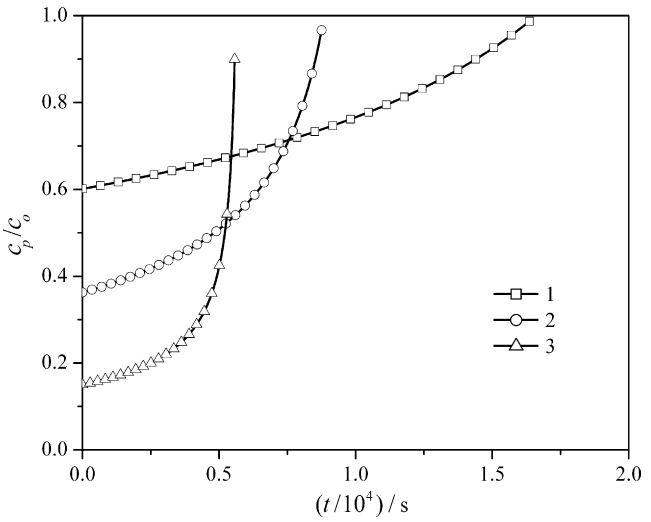

Fig. 6. Time dependences of electroactive ions concentration on the growing deposit surface at various overpotentials: (1) $\eta = -0.8$ V, (2) $\eta = -0.85$ V, and (3) $\eta = -0.91$ V.

Fig. 6 gives the time dependences of electroactive ion concentration on the growing deposit surface calculated by Eq. (20) at various overpotentials. It is seen that the initial dimensionless concentration of these ions c_p/c_0 increases with decreasing overpotential; the lower overpotential, the smaller is the deviation of concentration on the deposit surface from the bulk concentration. The higher overpotential, the higher is the rate of cation concentration variation on the growing deposit surface.

In Fig. 6, the initial concentrations are nonzero. This means that at the beginning of quasi-steady-state period of deposit growth in the pores, the diffusion limiting current was not reached.

Under different conditions, the limiting current can be reached even at the beginning of considered period of pore filling (this was assumed in several cited works). However, in the course of pore filling, the current can become lower than the limiting one due to a decrease of diffusion layer thickness.

Fig. 7 gives the plots of pore filling time vs. the overpotential at various concentrations c_0, which are calculated by Eq. (21). First, the filling time decreases and, then, becomes independent of overpotential corresponding to the diffusion limiting current.

At relatively low overpotentials, t_{fill} is virtually independent of the bulk solution concentration c_0 and is determined only by the overpotential. At high overpotentials, t_{fill} is determined by the electrolyte concentration c_0.

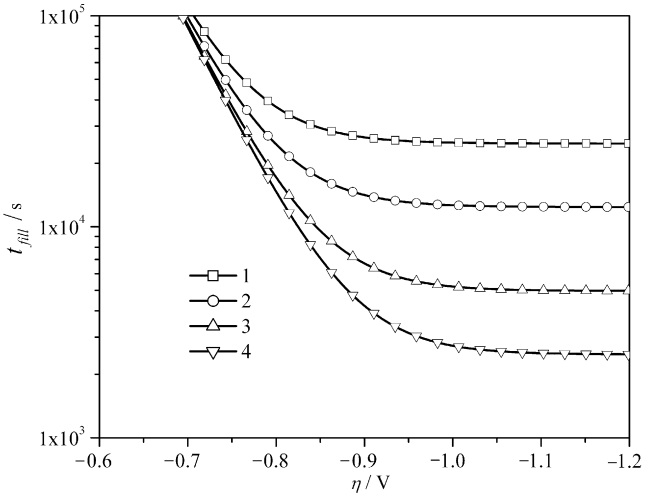

Fig. 7. The plots of pore filling time vs. the overpotential at various concentrations of electroactive ion c_0: (1) 0.1 M, (2) 0.2 M, (3) 0.5 M, and (4) 1 M.

5. Conclusions

The model of electrochemical growth of ordered arrays of high aspect ratio nanowires in the nonconducting template is developed. The initial non-steady-state period of the process is ignored, because its duration is by two orders of magnitude shorter than the pore filling time. It is taken into account that the metal deposition depends both on the conditions of metal cations diffusion and on the overpotential by the Tafel equation. The presence of outer diffusion layer above the template surface and a possible difference between the diffusion coefficients of electroactive ions in the inner diffusion layer (in the pore) and in the outer diffusion layer were taken into account. An approximation of uniform outer diffusion layer was used.

Within the model, the exact solution was obtained for the potentiostatic mode of metal deposition in the pores. With regard for the template porosity, the following characteristics of the process were obtained: the time dependences of current and concentration of electroactive ions at the growing deposit surface; the dependence of pore filling time on the overpotential of electrochemical reaction, etc.

An example of qualitative agreement between the calculated and experimental data is given. It is shown that an abrupt increase of the current in the curve of the current vs. the deposition time do not necessarily indicate that the metal wires emerge from the template surface.

However, the agreement between the calculated and experimental results in the above example does not mean that the model is sufficient for exact analysis of various experimental results. Therefore, the model for the growth of electrodeposits in the pores with a high aspect ratio should be further improved.

Acknowledgments

This work was supported by the Russian Foundation for Basic Research, project no. 13-03-00537.

References

[1] P.C. Searson, R.C. Cammarata, C.L. Chien, Electrochemical processing of metallic nanowire arrays and nanocomposites, Journal of Electronic Materials 24 (1995) 955.
[2] T. Nagaura, F. Takeuchi, Y. Yamauchi, K. Wada, S. Inoue, Fabrication of ordered Ni nanocones using a porous anodic alumina template, Electrochemistry Communications 10 (2008) 681.
[3] E. Quiroga-Gonzalez, E. Ossei-Wusu, J. Carstensen, H. Foll, How to make optimized arrays of Si wires suitable as superior anode for Li–ion batteries, Journal of the Electrochemical Society 158 (2011) E119.
[4] M.C. Lopes, C.P. Oliveira, E.C. Pereira, Computational modeling of the template-assisted deposition of nanowires, Electrochimica Acta 53 (2008) 4359.
[5] Y. Bai, Y. Sun, C. Sun, Pt–Pb nanowire array electrode for enzyme-free glucose detection, Biosensors and Bioelectronics 24 (2008) 579.
[6] X.W. Wang, Z.H. Yuan, S.Q. Sun, Y.Q. Duan, L.J. Bie, Thermal expansion behaviors of hcp and fcc Co nanowire arrays, Physics Letters A 373 (2009) 2887.
[7] M.P. Proenca, C.T. Sousa, J. Ventura, M. Vazquez, J.P. Araujo, Ni growth inside ordered arrays of alumina nanopores: enhancing the deposition rate, Electrochimica Acta 72 (2012) 215.
[8] D. Pullini, D. Busquets, A. Ruotolo, G. Innocenti, V. Amigo, Insights into pulsed electrodeposition of GMR multilayered nanowires, Journal of Magnetism and Magnetic Materials 316 (2007) e242.
[9] K. Rumpf, P. Granitzer, P. Polt, A. Reichmann, H. Krenn, Structural and magnetic characterization of Ni-filled porous silicon, Thin Solid Films 515 (2006) 716.
[10] C.-L. Xu, H. Li, G.-Y. Zhao, H.-L. Li, Electrodeposition and magnetic properties of Ni nanowire arrays on anodic aluminum oxide/Ti/Si substrate, Applied Surface Science 253 (2006) 1399.
[11] C.-L. Xu, S.-J. Bao, L.-B. Kong, H. Li, H.-L. Li, Highly ordered MnO_2 nanowire array thin films on Ti/Si substrate as an electrode for electrochemical capacitor, Journal of Solid State Chemistry 179 (2006) 1351.

[12] Z.-A. Hu, H. Wu, X. Shang, R.-J. Lu, H.-L Li, Template synthesis of $LaMnO_{3+\delta}$ (ordered nanowire arrays by converse diffusion or convection, Materials Research Bulletin 41 (2006) 1045.
[13] R. Inguanta, M. Butera, C. Sunseri, S. Piazza, Fabrication of metal nano-structures using anodic alumina membranes grown in phosphoric acid solution: tailoring template morphology, Applied Surface Science 253 (2007) 5447.
[14] L. Li, Y. Zhang, G. Li, X. Wang, L. Zhang, Synthetic control of large-area, ordered bismuth nanowire arrays, Materials Letters 59 (2005) 1223.
[15] J. Xu, X. Huang, G. Xie, Y. Fang, D. Liu, Fabrication and magnetic property of monocrystalline cobalt nanowire array by direct current electrodeposition, Materials Letters 59 (2005) 981.
[16] S. Cherevko, X. Xing, C.-H. Chung, Electrodeposition of three-dimensional porous silver foams, Electrochemistry Communications 12 (2010) 467.
[17] S. Valizadeh, J.M. George, P. Leisner, L. Hultman, Electrochemical deposition of Co nanowire arrays; quantitative consideration of concentration profiles, Electrochimica Acta 47 (2001) 865.
[18] R. Inguanta, S. Piazza, C. Sunseri, Novel procedure for the template synthesis of metal nanostructures, Electrochemistry Communications 10 (2008) 506.
[19] C. Jia, B. Zhang, W. Liu, L. Yao, W. Cai, X. Li, Single crystal Ag_7Te_4 nanowire arrays prepared by DC electrodeposition from aqueous solution, Journal of Crystal Growth 285 (2005) 527.
[20] K. Nielsch, F. Muller, A.-P. Li, U. Gosele, Uniform nickel deposition into ordered alumina pores by pulsed electrodeposition, Advanced Materials 12 (2000) 582.
[21] Q. Wang, Electrochemical template synthesis of large-scale uniform copper selenides nanowire arrays, Materials Letters 63 (2009) 1493.
[22] Y.-W. Yang, Y.-b. Chen, F. Liu, X.-y. Chen, Y.-c. Wu, Template-based fabrication and electrochemical performance of CoSb nanowire arrays, Electrochimica Acta 56 (2001) 6420.
[23] X.W. Wang, Z.H. Yuan, J.S. Li, (1 1 0) Orientation growth of magnetic metal nanowires with face-centered cubic structure using template synthesis technique, Materials Characterization 62 (2011) 642.
[24] Y. Chen, Y. Yang, X. Chen, F. Liu, T. Xie, Orientation-controllable growth of Sb nanowire arrays by pulsed electrodeposition, Materials Chemistry and Physics 126 (2011) 386.
[25] H. Liu, B. Lu, S. Wei, M. Bao, Y. Wen, F. Wang, Electrodeposited highly-ordered manganese oxide nanowire arrays for supercapacitors, Solid State Sciences 14 (2012) 789.
[26] J.M. Montero-Monero, M. Belenguer, M. Sarret, C.M. Muller, Production of alumina templates suitable for electrodeposition of nanostructures using stepped techniques, Electrochimica Acta 54 (2009) 2529.
[27] R. Alkire, D. Ernsberger, D. Damon, The role of conductivity variations within artificial pits during anodic dissolution, Journal of the Electrochemical Society 123 (1976) 458.
[28] I.U. Schuchert, M.E. Toimil Molares, D. Dobrev, J. Vetter, R. Neumann, M. Martin, Electrochemical copper deposition in etched ion track membranes, Journal of the Electrochemical Society 150 (2003) C189.
[29] H. Gomez, G. Riveros, D. Ramirez, R. Henriquez, R. Schrebler, R. Marotti, E. Dalchiele, Growth and characterization of ZnO nanowire arrays electrodeposited into anodic alumina templates in DMSO solution, Journal of Solid State Electrochemistry 16 (2012) 197.
[30] T.M. Whitney, J.S. Jiang, P.C. Searson, C.L. Chien, Fabrication and magnetic properties of arrays of metallic nanowires, Science 261 (1993) 1316.
[31] S.Z. Chu, S. Inoue, K. Wada, K. Kurashima, Fabrication of integrated arrays of ultrahigh density magnetic nanowires on glass by anodization and electrodeposition, Electrochimica Acta 51 (2005) 820.
[32] L. Piraux, S. Dubois, S. Demoustier-Champange, Template synthesis of nanoscale materials using the membrane porosity, Nuclear Instruments and Methods in Physics Research Section B 131 (1997) 357.
[33] R.T. Bonnecaze, N. Mano, B. Nam, A. Heller, On the behavior of the porous rotating disk electrode, Journal of the Electrochemical Society 154 (2007) F44.
[34] K.S. Napolskii, I.V. Roslyakov, A.A. Eliseev, D.I. Petukhov, A.V. Lukashin, S.-F. Chen, C.-P. Liu, G.A. Tsirlina, Tuning the microstructure and functional properties of metal nanowire arrays via deposition potential, Electrochimica Acta 56 (2011) 2378.
[35] K.S. Napolskii, P.J. Barczuk, S.Yu. Vassiliev, A.G. Veresov, G.A. Tsirlina, P.J. Kulesza, Templating of electrodeposited platinum group metals as a tool to control catalytic activity, Electrochimica Acta 52 (2007) 7910.
[36] V.V. Korotkov, V.N. Kudryavtsev, D.L. Zagorskii, S.A. Bedin, Electrodeposition of cobalt in micro- and nano-sized pores of polymer ion-track membranes, Plating and Surface Finishing 19 (4) (2011) 23 (in Russian).
[37] D. Almawlawi, N. Coombs, M. Moskovits, Magnetic properties of FE deposited into aluminum oxide pores as a function of particle size, Journal of Applied Physics 70 (1991) 4421.
[38] E.A. Bluhm, E. Bauer, R.M. Chamberlin, K.D. Abney, J.S. Young, C.D. Jarvinen, Surface effects on cation transport across porous alumina membranes, Langmuir 15 (1999) 8668.
[39] E.A. Bluhm, E. Bauer, J.N. Fife, R.M. Chamberlin, K.D. Abney, J.S. Young, C.D. Jarvinen, Surface effects on cation transport across porous alumina membranes. 2. Trivalent cations: Am, Tb, Eu, and Fe, Langmuir 16 (2000) 7056.
[40] W.D. Williams, N. Giordano, Fabrication of 80 Å metal wires, Review of Scientific Instruments 55 (1984) 410.
[41] G.R. Engel'gardt, A.D. Davydov, T.B. Zhukova, H.-H. Strehblow, New description of mass transport in electrochemical reactions at the bottom of cylindrical channels, Soviet Electrochemistry 28 (1992) 199.
[42] A.M. Sukhotin (Ed.), Handbook of Electrochemistry, Khimiya, Leningrad, 1981.